ORIGINAL RESEARCH ARTICLE

DOI: https://doi.org/10.18599/grs.2018.4.344-354

The safe operations modes substantiation for water source wellbores of the Vadelypskoye deposit

A.V. Seryakov[1], M.Yu. Podberezhny[2], O.B. Bocharov[1], M.A. Azamatov[2]*

[1]*Novosibirsk Technology Center Baker Hughes JSC, Novosibirsk, Russian Federation*

[2]*Salym Petroleum Development N.V., Moscow, Russian Federation*

Abstract. The sand production problem for the water sources wellbores at the Vadelypskoye oilfield that is located in Hanty-Mansy region of Russia is considered. The serious issue during field operations is the open wellbore wall destruction even if low drawdown rates (4-6 bar) are applied to the water-bearing pay at one kilometer depth.

Petrophysical analysis of high permeable (0.6-2.5 D) sandstones of water-bearing pay is presented. The effectiveness of the sands prevention methods used at the deposit is discussed and the practical recommendations for drilling and operations are given.

To identify the conditions of safe fluid extraction the three-dimensional poroelastic software was used for modeling of the vertical borehole section located in the water saturated sandstone. We consider the mudcake is stripped and disappeared due to the wellbore technological operations but the plugging zone persisted. The colmatage zone was taken into account in the modeling as the radial area with reduced relative to formation permeability. Along with this, the axial sandstone permeability is non-uniform and assigned according to the core data.

Different horizontal stresses ratios and values are considered in the simulations. The medium-clogged and high-clogged damage zone influence on the formation effective stresses was studied for minimal and maximal drawdown values. It was established that the most stable borehole relative to the draw-down is located in the homogeneous horizontal stress field within the medium-clogged damage zone.

Special attention was given to the damage zone permeability and thickness influence on the wellbore wall failure while pumping. It was determined that rock failure is more possible when the thin and low-permeable colmatage zone is built in formation. The near-wellbore zone colmatage effect on rock destruction can be definitely seen for conditions of equal horizontal stresses but decreases when horizontal loads are unequal. The analysis of different in-situ conditions showed that the difference between horizontal stresses has more effect on destruction than colmatage zone parameters changes.

The water-pumping admissible drawdown pressure ranges are specified for each horizontal stresses regime and the recommendations were given for sanding screen characteristics. For wellbore planning at the Vadelypskoye deposit the preferable drill mud composition was described that will contribute to subsequent safe water pumping.

Keywords: sand production, water sources wellbores, destruction, poroelastic modelling, high permeable sandstone, colmatage zone

Recommended citation: Seryakov A.V., Podberezhny M.Yu., Bocharov O.B., Azamatov M.A. (2018). The safe operations modes substantiation for water source wellbores of the Vadelypskoye deposit. *Georesursy = Georesources*, 20(4), Part 1, pp. 344-354. DOI: https://doi.org/10.18599/grs.2018.4.344-354

Introduction

One of the problems occurring hydrocarbon displacement by water is formation failure while water production from weak sandy sediments. Apart from damaging the equipment, sand production causes data transfer problems due to the hydrodynamic telemetry channel clogging while drilling. Therefore determining of the critical parameters and events that prevent sand production is a main issue.

At the Vadelypskoye oil field water production is performed from the upper (relative to oil reservoirs) layers mainly composed of highly permeable sandstones (600-2500 mD). What raises a red flag is that sand production starts at relatively low-pressure drawdown changing within 4-6 bar.

This paper presents the petrophysical characteristics of the water-saturated sandbody. It discusses the effectiveness of the methods that prevent sand particles from getting into the lifted water. It also presents the

*Corresponding author: Alexander V. Seryakov
E-mail: Alexander.Seryakov@bakerhughes.com

© 2018 The Authors. Published by Georesursy LLC
This is an open access article under the CC BY 4.0 license
(https://creativecommons.org/licenses/by/4.0/)

results of 3D numerical geomechanical modeling of the water-supply sections of the sandbody that have become a basis for determining safe pressure-drop ranges to minimize formation failure. In addition, the article gives recommendations on the composition of drilling muds to reduce sand production at the Vadelypskoye oil field.

Description of the oil field

The Salym oil fields are located 120 km from Surgut in Khanty-Mansi Autonomous Area and operated by the Salym Petroleum Company (SPD). The Vadelypskoye field borders on West Salym and Upper Salym fields (Fig. 1). The field's geological structure composed of a Paleozoic folded basement, an intermediate complex and the terrigenous sandy-argillaceous sediments and a Mesozoic-Cenozoic platform mantle. Its commercial oil inflow comes from the Cherkashin and the Achimov units.

To maintain the sufficient formation pressure necessary for efficient oil displacement the company uses water flooding, in particular, injecting the Aptian-Albian heterolitics (Uvat formation) underground waters, whose average mineralization (17 g/l) is similar to the one of oil reservoir water. The issues of application of formation pressure maintenance (FPM) systems at the field is maintaining the stability of the walls of uncased water-supply wells and sanding during water lift from the Uvat formation, whose average thickness is about 290 m. Most of the formation (85%) is permeable sediments (Fig. 2) with the water reservoirs mainly formed of

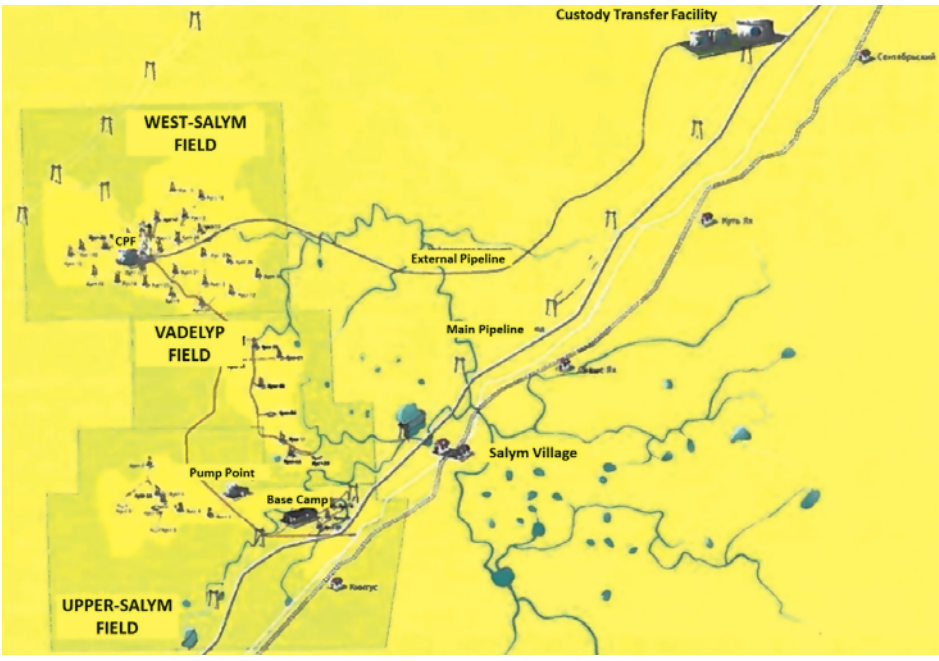

Fig. 1. Map of the Salym oil fields

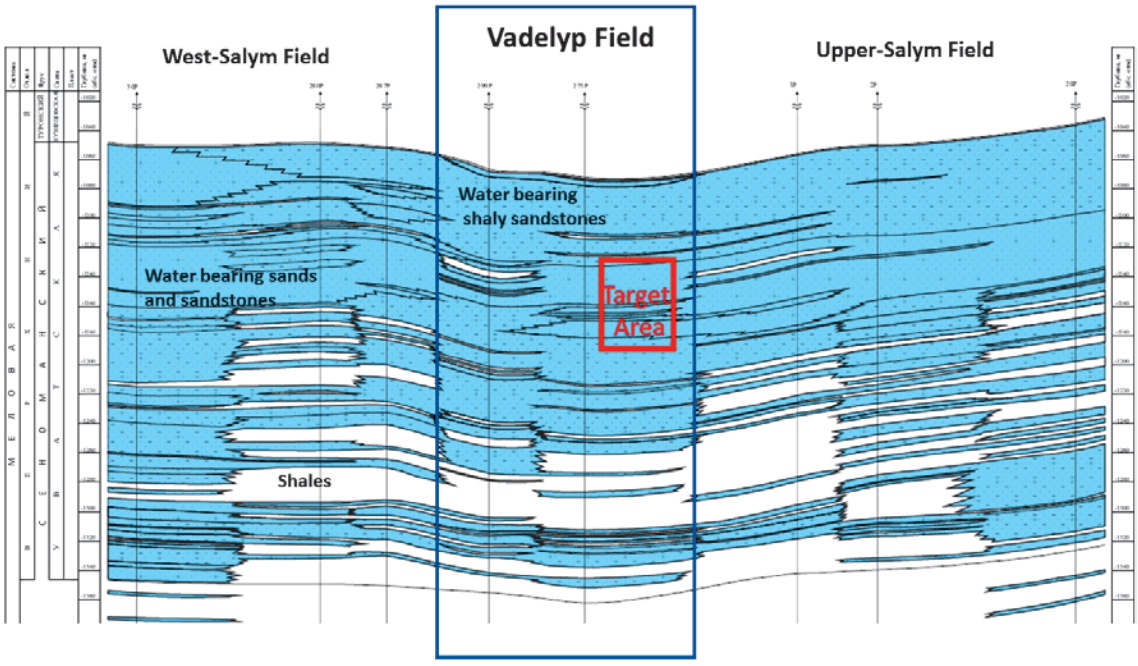

Fig. 2. The Aptian-Albian heterolitics of the Salym oil fields. The red box marks the location of the hole

siltstone (55%); sand and silt rocks, and sandstone present in 30% and 16 % respectively.

Petrophysical analysis of a core from the water-saturated layer of the Uvat formation, taken at the depth of about 1 km showed the presence of thin carbonate interlayers in the sandstone as well as the presence of siltstone (Fig. 3).

Most of the volume in the studied interval was sandstone to be a consolidated, but relatively fragile rock that being drilled produces high amounts of suspended particles, which trouble data transfer while drilling.

Methods to prevent sand production

Traditionally sand production and falling of the macrofracmental pieces of rock in a well is prevented by installation of different protective devices that reduce the well-head erosion and downhole equipment damage in operation. Selecting a proper protective system requires an R&D study to maximize the effectiveness of the protection.

At the Vadelypskoye oil field, they install suspended wire-wrapped sand screens with different cell sizes. It has been confirmed that the cells of 0.2 mm (200 μm) the concentration of transported particles is 75 mg/l. In this case, the main part of the sediment is grains of 60-100 μm as shown in Table 1.

Field measurements and analysis of the volume ratio of transported sand particles have shown that sand screen with the cells of 0.1 mm (Fig. 4) reduces particle concentration 7 times to 10 mg/l.

Reducing the cell size to 0.05 mm has resulted in complete clogging of the screen and water lift termination, so optimal formation – fluid filtration occurs through the cells of 0.1 mm in size.

Grain size, μm	Portion in the sample, %
7.5-20	5
20-60	25
60-100	60
>100	10

Table 1. Sand particle size distribution

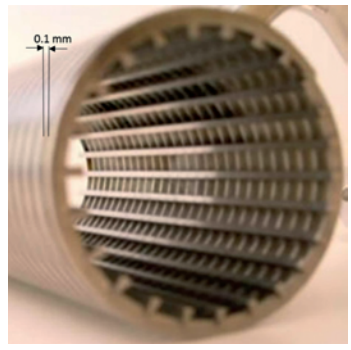

Fig. 4. Wire-wrapped sand screen with the cell width of 0.1 mm

Logging and petrophysical core analysis data

The water-bearing level of the well we considered in our study was located within the depths of 1247-1257 m. Within this interval, the SibBurMash Company performed an isolated coring procedure. The core samples were fixed in transportation cases with a polymer composition to prevent their possible damage while moving to the laboratory. After the coring, the Kogalymneftegeofizika (KNGF) Company ran a combo wireline logging tool including gamma (GR), microlog (MPZ, MGZ), caliper, density (RHOZ), neutron (TNPH), five-probe induction (AE10-90) and acoustic logging (VP) devices. The results of the described procedures can be seen in Fig. 5.

In the laboratory of Coretest Services Company, the core was measured and a standard set of analyses was

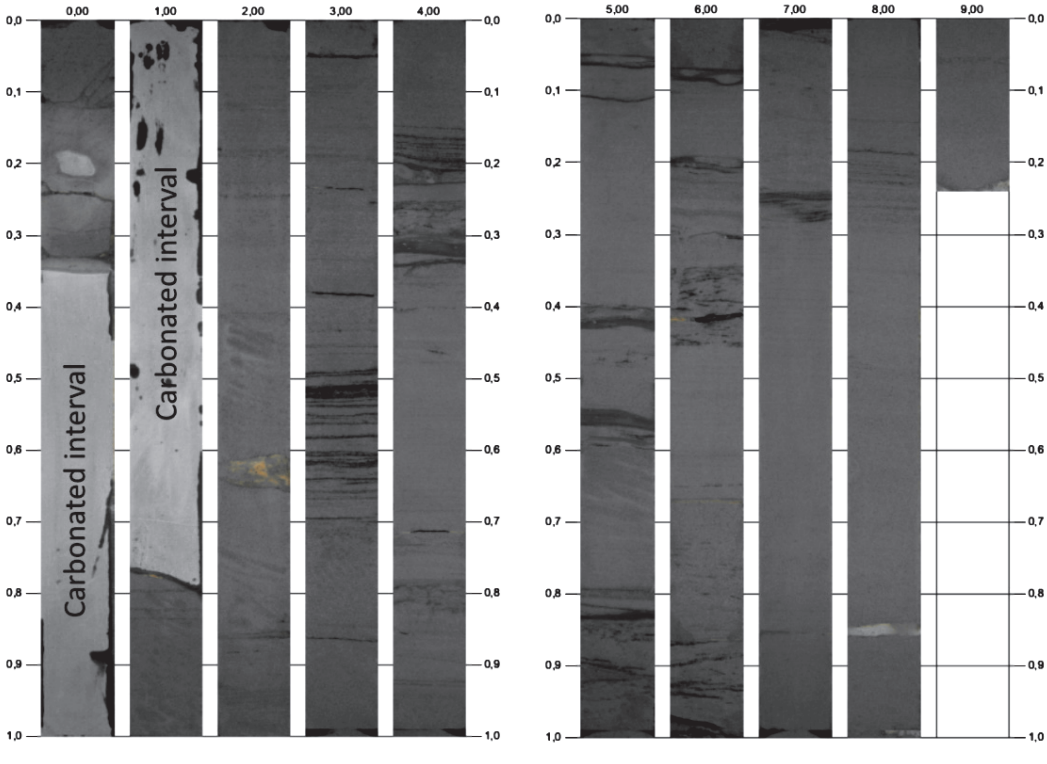

Fig. 3. Day-light photograph of one-meter sections of the core extracted from the water-bearing layer of the Uvat formation

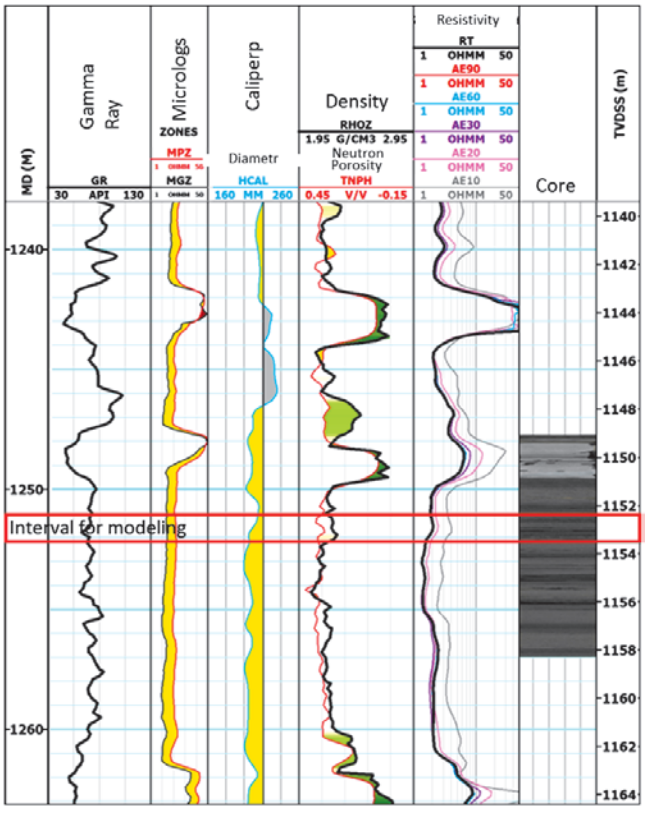

Fig. 5. Logging and coring results. The red box marks the interval selected for modeling

performed including studying the core's granulometric composition and geomechanical tests for formation conditions to determine steady and dynamic elasticity moduli, and breakdown moduli.

The tests demonstrated the core's average porosity to be 33% and permeability – 875 mD. The reservoir's minimum porosity value was 17% and permeability – 0.4 mD. Measurements of the porosity ϕ and permeability *k* showed a very good match with the regional (West Siberia) trend: $Log_{10}(k) = 21.36 \cdot \phi - 4.15$ (Fig. 6).

Thin-section analysis demonstrated the rock within the indicated interval to be fine-grained sandstone with finely cemented quartz grains of subrounded shape. The

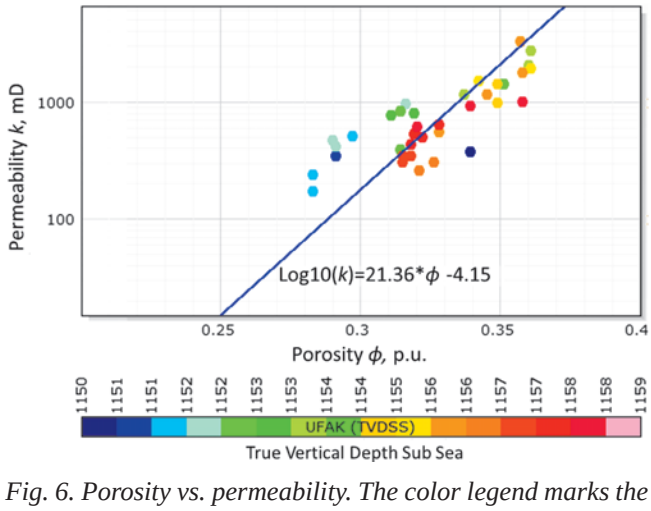

Fig. 6. Porosity vs. permeability. The color legend marks the absolute depth in meters

grains, as a rule, do not have clear orientation and their disposition is chaotic. Measuring orthogonal S-waves (VS1, VS2) in a water-saturated core also revealed no anisotropy (Fig. 7) and confirmed the rock structure as appropriate for isotropic description at micro-, meso- and macrolevels.

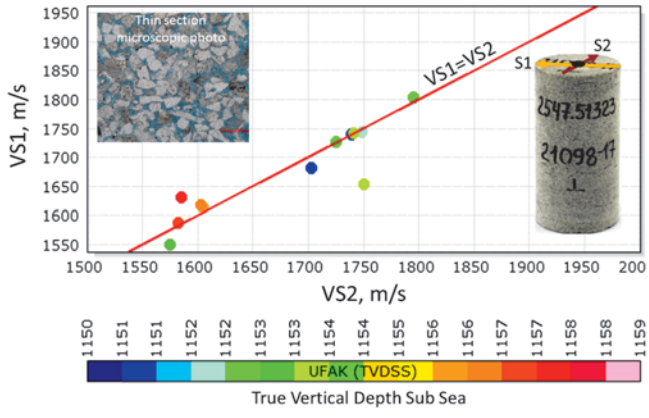

Fig. 7. Measured orthogonal S-wave velocities and the thin section demonstrate the rock's isotropy. The color legend marks absolute depths in meters

Porous medium deformation model

To develop a strategy for drilling and operation of water-supply wells that have no casing within the productive interval, 3D geomechanical modeling of the water-supply layers was performed.

The joint changes of stresses and pore pressure in a formation is described with the quasi-static Biot model (Biot, 1941; Biot, Willis, 1957), whose equation system includes equilibrium equations for the total stress tensor σ_{ij}:

$$\sigma_{ij,j} = g_i \,. \tag{1}$$

The comma in the equation indexes denotes a corresponding coordinate derivative, $\vec{g} = (0,0,\rho g)$.

The momentum conservation equation with the Darcy law results in the equation for pore pressure p:

$$\frac{1}{M}\frac{\partial p}{\partial t} - \frac{k}{\mu}\Delta p + \alpha\frac{\partial e}{\partial t} = 0, \tag{2}$$

where *e* denotes the volumetric deformation, *M* – the Biot modulus, *k* – the medium permeability, μ – the fluid viscosity, α – the Biot-Willis coefficient.

The physical ratios between total stresses, deformations and pore pressure are expressed through generalized Hook's law. In assumption of isotropic medium, these ratios are written as:

$$\sigma_{ij} = 2G\varepsilon_{ij} + \lambda e\delta_{ij} - \alpha p, \tag{3}$$

where *G* denotes the shear modulus, λ – the Lame parameter, ε_{ij} – deformation tensor components. As the destruction criterion, the model relies upon The Mohr-Coulomb failure criterion, which means a failure is initiated when the value of equivalent stress function σ_e

determined from equation (4) exceeds the unconfined compressive strength (UCS):

$$\sigma_e = \sigma_1' - \sigma_3' ctg\psi, \quad (4)$$

where σ_1', σ_3' denote the minimum and maximum main effective stress, $ctg\psi = (1+\sin\varphi)/(1-\sin\varphi)$, φ – the inner friction angle.

The equation system (1)-(3) in solved in 3D space using the finite – element method (Zienkiewicz, 1971; Wang, 2000). Hexagons are used to discrete the continuous medium. The basic functions are determined for the hexagon's apexes and are bilinear, while the shape functions are quadratic, which allows one to describe a well's surface. The numerical algorithm to solve poroelastic problem conjugates the solution for the pore pressure and for displacement trough iterations at each time step until a given accuracy for determined parameters is achieved (Manakov, 2012).

The finite-element algorithm has been implemented in the Geofluid 3D software package that also includes a mesh generator, a solver and a post processor.

Input modeling parameters

For modeling purposes, we selected a one -meter interval (1252.55-1253.55 m) of an uncased well with the radius of r_b = 0.11 m and the formation permeability k changing in accord with the permeability profile (Table 2).

Within the selected borehole interval cores were taken perpendicular to the bedding at the depths of 1252.34, 1252.56 and 1253.06 meters. The core samples were studied in a laboratory to determine the porosity φ and the static elastic modules (Young modulus E, Poisson' s ratio and UCS) that were obtained from a triaxial compression test for the reservoir conditions.

The computation domain was a one-meter vertical formation section around a well, surrounded by a mesh (Fig. 8). The rock's poroelastic properties were considered constant for the whole section apart from the permeability k, whose values changed in accordance with Table 2.

Depth, m	k, mD
1252.55	1992.86
1252.60	1027.21
1252.65	1222.66
1252.75	1244.95
1252.80	2110.56
1252.85	1513.01
1252.90	1530.42
1252.95	1444.12
1253.00	2053.87
1253.05	1740.98
1253.10	1152.60
1253.15	811.16
1253.20	1539.87
1253.25	0.39
1253.30	1705.04

Table 2. Permeability profile of water-saturated interval

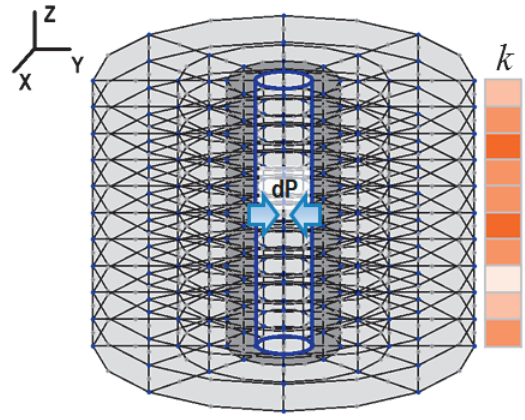

Fig. 8. Computation domain

The obtained logging and coring data were used to determine the input parameters of modelled interval presented in Fig. 9. For the Vadelypskoye – field rock the shear modulus values is $G = E/2(1+\nu)$ = 2.07 GPa, and the Biot-Willis coefficient α = 0.95. The granule compressibility of the rock matrix was selected to be K'_s = 36 GPa, which is a characteristic compressibility value for sandstones (Wang, 2000); and fluid compressibility K_f = 2.3 GPa for water. Using the formula derived from the poroelasticity equations (Bocharov, Seryakov, 2016):

$$K_u B = \frac{K_s'}{\phi(c_f/\delta - 1)} = \frac{K_s'}{\phi(K_s'/K_f - 1)}, \quad (5)$$

where the porosity $\phi = 0.34$, we obtained K_uB = 7.23 GPa and derived the Biot parameter $M = K_uB/\alpha$ = 7.64 GPa.

A pressure drop (dP) being a difference between formation and borehole pressures was set on the borehole wall. In case of water pumping this parameter becomes negative, but here in the article, we are going to use its positive values and to underline that we are dealing with a pressure drawdown scenario. In order to account for a mud damaged zone or a colmatation zone, the formation permeability along the radial coordinate was considered heterogeneous. The colmatation zone was marked as a shaded area around the well (Fig. 10).

The caliper measurements performed in 8 hours after penetration had shown a presence of mudcake whose thickness varied from 10 to 15 mm. Since the studied sandstone was of highly-permeable type, the creation of a damaged zone did not cause any doubts. When modeling water pumping we assumed that all the mudcake was washed out while drillstring tripping, so only a colmatation zone with the thickness h_d, and reduced, relative to the formation, permeability k_d was accounted for (Fig. 3). It was apparent that the near-wellbore zone contamination degree characterized by

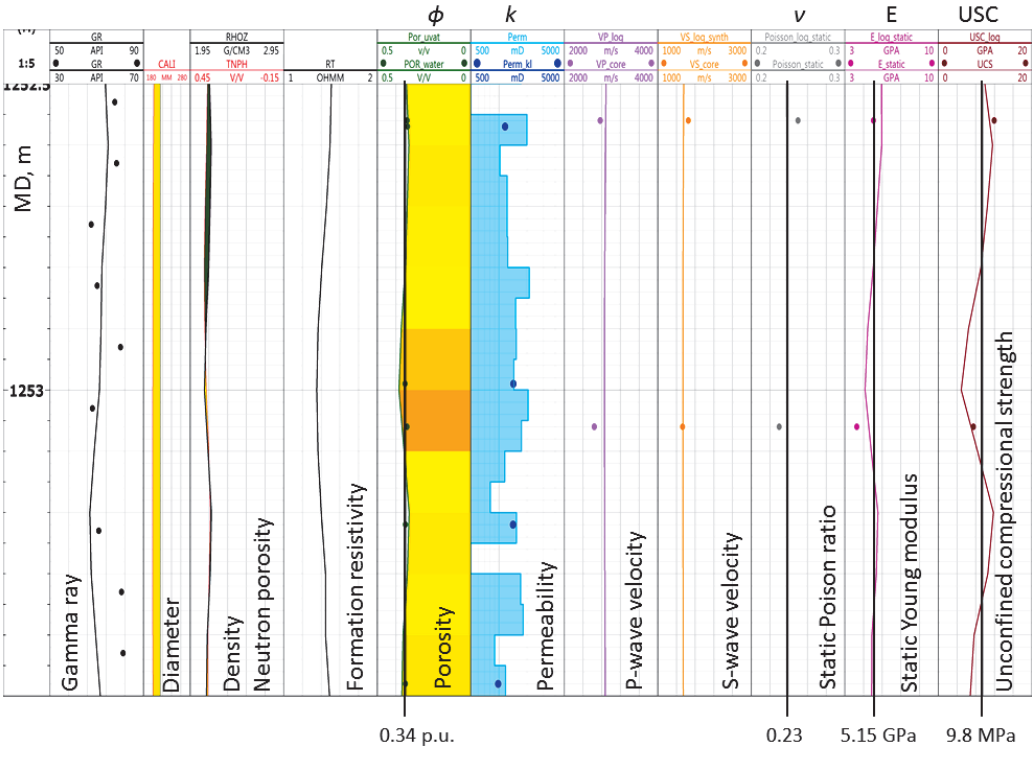

Fig. 9. Logging data and interpretation results; coring and the average parameter values used in the modeling

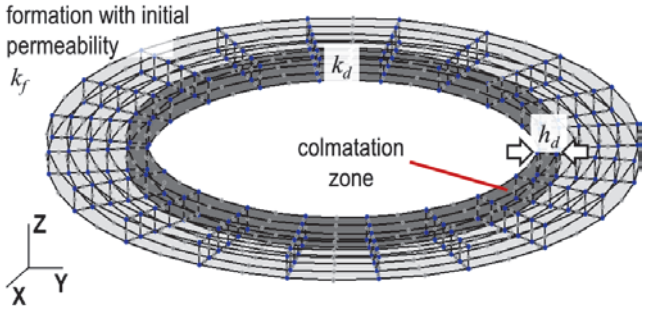

Fig. 10. Near-well area schematic. The colmatation zone has thickness h_d and permeability k_d that is the fraction of the total formation permeability k at the given depth

the parameters k_d and h_d would play important role in the distribution of pore pressure and, consequently, effective stresses around the well. In order to forecast the well's behavior, its stability parameters had been calculated for different experimentally confirmed near-well parameters (Podberezhny et al., 2017). For the computations parameter h_d was varied from 2 to 30 mm, parameter k_d was varied from 0.1 to 0.0001 of the formation permeability beyond the colmatation zone *k*.

Now, let us consider initial geomechanical conditions around the well. The pore pressure *p* in the formation was 12.3 MPa, which was confirmed by field data and corresponds to hydrostatic. The vertical stress S_v calculated from gamma-gamma density logging data was 23 MPa for the given depth. The estimations of the minimum horizontal stress напряжения S_{hmin} were within the range of 15-17.5 MPa, which was confirmed by DFIT data. As for the maximum horizontal stress S_{Hmax}, downhole measurements showed it could be as equal to the minimum or inline from it by the value up to 1 MPa.

One of the most important parameter for borehole wall stability modeling is UCS. Considering the parameter's distribution within the 1252.55-1253.55 m interval, a conclusion was made that its lowest value would correspond to the highly – permeable sublayer at the depth of 1253 m where the highest porosity level (34%) increased the probability of matrix damage and sanding.

According to the results of laboratory core studies (Fig. 11), the UCS and porosity correlated as $UCS = 277 \cdot e^{-10 \cdot \phi}$, which corresponds to the data provided by Chang et al, 2006. Considering the assessment data, in our study we had decided to use the value UCS = 9.8 MPa to determine breakdown in the highly-permeable interval.

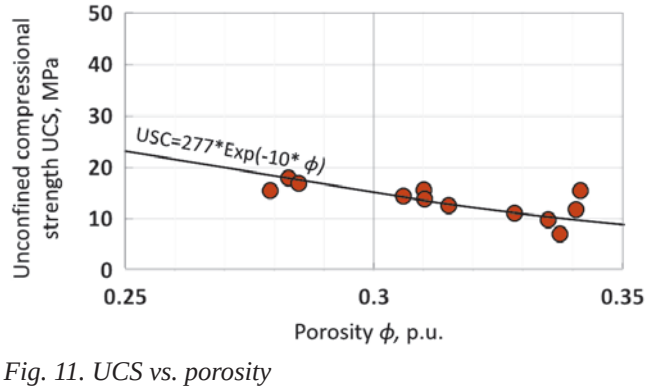

Fig. 11. UCS vs. porosity

Results of the modeling

Here it should be underlined one more time that the main objective of the modeling was determining of safe water pumping modes within previously described ranges for minimum and maximum horizontal stresses, in dependence of pump-off pressure and near-well contamination degree.

A. Downhole conditions and admissible pressure drawdown

First hand, we studied the effect the horizontal stresses and pressure drawdown degree had on sand production. To determine the main regularities of the stress state in computations for different colmatation zones some extreme values were selected: 0.2*k* that is often used in commercial packages (GMI SFIB User's manual, 2008) and 0.001*k*, where *k* denotes formation permeability. For the maximum horizontal stress S_{Hmax} and minimum S_{hmin} the following options were considered:

1(A): when the stresses were equal $S_{Hmax} = S_{hmin}$ with the extreme stress values S_{hmin} = 15 MPa and S_{hmin} = 17.5 MPa studied;

2(A): when $S_{Hmax} = S_{hmin}$+1 MPa with the boundary stress values S_{hmin} = 15 MPa, S_{Hmax} = 16 MPa; S_{hmin} = 7.5 MPa, S_{Hmax} = 18.5 MPa studied.

During modeling, the boundary *dP* values of 4 and 6 bar were used.

At the preliminary stage of the computations, it was found out that the stress function value σ_e (equation 4) changes insignificantly along the well's trajectory. The qualitative representation of this phenomenon can be seen in Fig. 12 (a) demonstrating a 2D distribution pattern of σ_e where on z-axis is plotted the relative depth h whose zero value corresponds to the upper sandstone boundary of 1252.5 m.

For detailed estimation of σ_e it was more convenient to consider 1D depth-related plot presented in Fig. 12 (b). Modeling was performed for the following conditions: $S_{Hmax} = S_{hmin}$ = 15 MPa, *dP* = 4 bar and 5-mm radius of the damaged zone with the permeability equal to 0.001 of the formation permeability. As you can see the measurement of σ_e can be described with a linear function, except for an interval at the relative depth of h = 0.7 m. Comparing this deviation with the permeability distribution given in Fig. 12 (c) one can see the presence of a low-permeable carbonate interlayer. However, this deviation amplitude is less than 1%, while from a solid interlayer one usually expects a significant UCS increase. For that reason, when estimating the rock failure, we regarded an interval at the relative depth of 0.5 m where maximum porosity, permeability and UCS were reached.

Variant 1(A). Results obtained for equal stresses $S_{Hmax} = S_{hmin}$.

It was established that at the pressure drop of 4 bar rock failure occurs only when $S_{Hmax} = S_{hmin}$ = 15 MPa in low-permeable colmatation zone, in other words, when k_d. = *0.001k*. In this case, the maximum σ_e value of 9.92 MPa was registered not on the well contour but at the distance of about 2 mm from its walls. This change of the function σ_e was of regular character and revealed itself in the low-permeable colmatation zones. We will touch on this effect in more detail in the part describing the effect k_d and h_d have on well stability. When increasing the horizontal stresses up to

$S_{H\max}, S_{h\min}$, MPa	dP, bar	σ_e for $k_d = 0.2k$	σ_e for $k_d = 0.001k$	σ_e for $h_d = 0$
15	4	9.59	9.92	9.58
15	6	9.68	10.35	9.66
17.5	4	9.62	9.76	9.57
17.5	6	9.9	10.1	9.84

Table 3. The maximum values of σ_e (MPa) in the near-well area for homogeneous horizontal stresses

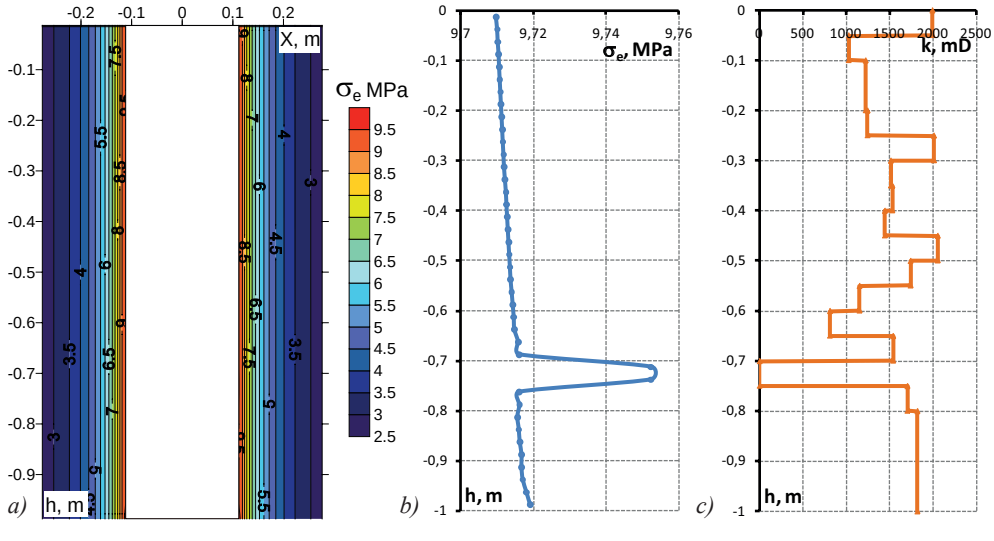

Fig. 12. Stress function (σ_e) distribution along the well: 2D spectral pattern (a);1D depth-related plot (b); formation permeability (c)

S_{Hmax} = S_{hmin} = 17.5 MPa, the failure occurs neither at k_d = 0.001k nor at k_d = 0.2k.

When water lift was performed at the pressure drawdown of 6 bar, the well remained intact only at S_{Hmax} = S_{hmin} = 15 MPa and k_d = 0.2k, while all the other combinations were unsafe. For more detail turn to Table 3, whose first two columns contain downhole conditions, and the other three – corresponding σ_e values.

In order to obtain a reference value for σ_e we calculated such water-lift variations that had no colmatation zone. The values of equivalent stress σ_e^0 for this case can be found in the utmost-right column of Tab. 3. Comparison σ_e^0 against the other calculated variants showed that the stress-state function in the colmatation zone with the permeability reduced down to 20% of the formation's has little difference from the values obtained for a water extraction from noncontaminated formation. This effect has been observed for the indicated low-pressure drawdown and initial stress ratio ranges in the formation. The modeling also demonstrated that the safest pump-off technique was pumping from a noncontaminated formation, which was impossible in presence of highly-permeable sandstones.

The colmatation zone with the permeability of 0.1% of the formation's was the reason for a more abrupt pressure drop in the contaminated area and increased near-well effective stresses.

The isolines and spectral diagrams of σ_e distribution in XY plane at the relative depth of 0.5 m for a case of homogeneous horizontal stress can be seen in Fig. 13.

Variant 2(A). As the deformation theory predicts, in a heterogeneous field of the horizontal loads $S_{Hmax} > S_{hmin}$, the maximum concentration of shear stresses went in the direction of the minimum stress S_{hmin}.

The σ_e values obtained for all the colmatation zone permeabilities and pressure drops exceeded the UCS value. Therefore, in the case of heterogeneous horizontal stresses, even with a slight difference the sand production begins. The numerical values of σ_e for the different initial conditions can be found in Table 4. Its last column contains the maximum values of σ_e^0 with no colmatation zone.

S_{hmin}, MPa	$S_{H\max}$, MPa	dP, bar	σ_e for $k_d = 0.2k$	σ_e for $k_d = 0.001k$	σ_e for $h_d = 0$
15	16	4	9.9	10.04	9.9
15	16	6	9.99	10.47	10
17.5	18.55	4	12.52	12.65	12.59
17.5	18.55	6	12.79	12.99	12.86

Table 4. The maximum values of σ_e (MPa) in the near-well area for heterogeneous horizontal stresses

Analysis of the obtained values showed that the presence of a colmatation zone with the permeability of 20% of the formation's even insignificantly reduce the level of equivalent stress in absence of rock breakdown. On the other hand, the low-permeable colmatation zone (0.1% of the formation's) increased the σ_e values. Comparing the σ_e values for the noncontaminated formation with their analogs from Table 3, we concluded that the horizontal-stress heterogeneity had a greater effect on a failure possibility than the colmatation zone parameters.

In Fig. 14 you can see the σ_e parameter distribution for the pressure drop of 4 bars and the borehole conditions S_{Hmax} = 18.55 MPa, S_{hmin} = 17.5 MPa.

Generalizing the results obtained for homogeneous and heterogenous horizontal stress it can be concluded

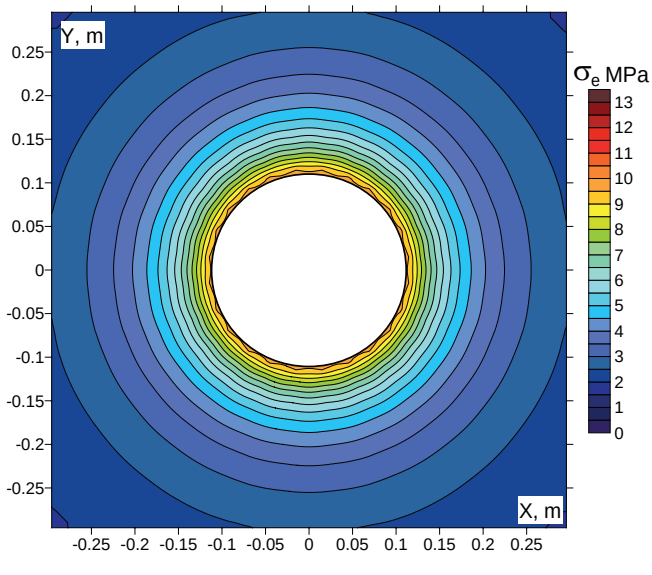

Fig. 13. Stress function σ_e distribution in the near-wellbore area calculated for S_{Hmax}=S_{hmin}=15 MPa, 4-bar pressure drop and colmatation zone k_d=0.001k. The horizontal section goes through an interlayer with highest permeability

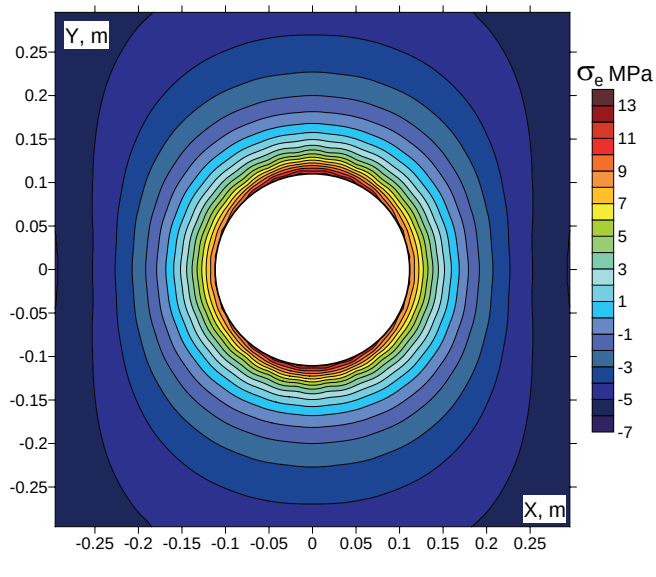

Fig. 14. Stress distribution (σ_e) in the near-welbore area, calculated for the pressure drop of 4 bar, the borehole conditions S_{Hmax}=18.55 MPa, S_{hmin} =17.5 MPa, and the colmatation zone permeability k_d = 0.001k

that a failure probability increases with increase in the amplitude and a difference between the horizontal stresses, with increase in pressure drawdown, and with reduction in the colmatation-zone permeability.

B. Invaded zone parameters and their effect on sand production

For further analysis of the colmatation zone effect on sandstone destruction during water pumping, we performed a series of computations with changing k_d (permeability) and h_d (width). The pressure drop was selected to be 4 bar and 2 variants of horizontal pressures were considered:

1(B): $S_{Hmax} = S_{hmin} = 16$ MPa;

2(B): $S_{Hmax} = 18.55$ MPa, $S_{hmin} = 17.5$ MPa.

For the colmatation zone width h_d the following values were set: 2, 5, 7, 10 and 30 mm. The colmatation zone permeability k_d varied from 10% to 0.01% of the formation's, that means that the coefficient γ in the ratio $k_d = \gamma k$ was 0.1, 0.01, 0.001 and 0.0001.

Variant 1(B). In the homogeneous field of horizontal stresses, a computation in absence of the colmatation zone gave $\sigma_e^0 = 9.558$ MPa. For analysis of the computations with colmatation zone taken into account it was convenient to consider the deviation function $\Delta\sigma_e = (\sigma_e - \sigma_e^0)/\sigma_e^0$ from the σ_e^0 reference value. The modeling demonstrated that the maximum level of equivalent stress was achieved in presence of a very small and low-permeable colmatation zone densely packed with drilling-mud particles. Under these conditions, water pumping induces a significant gradient of effective stresses that results in a breakdown. The $\Delta\sigma_e$ deviation distribution in dependence on the parameters of h_d and the reduction factor γ can be seen in Fig. 15.

Here it should be noted that a maximum stress value for the impermeable colmatation zone (0.1 and 0.01%) was obtained not on the borehole's wall, but in the formation at the distance of 1-2 mm from the well contour. This can be seen in the σ_e distribution diagrams built for the colmatation zone thickness of 2 and 5 mm (Fig. 16). So, if while water extraction UCS values are exceeded, rock failure is most likely to occur in the zone of 1-2 mm from the borehole wall.

In general, the modeling demonstrated that the invaded zone had a little effect on the stresses' degree in the pore matrix while water lift. Their highest increase (5%) was observed when a low-permeable and low-extended colmatation zone was formed.

Variant 2(B). In case of no colmatation zone, the maximum value of the equivalent stress σ_e^0 equal to 10.4841 MPa was obtained on the well contour in the direction of minimum horizontal stress. Therefore, the borehole conditions with $S_{Hmax} = 18.55$ MPa and $S_{hmin} = 17.5$ MPa are unsafe.

As the modeling shown the presence of invaded zone for heterogeneous horizontal stresses led to insignificant increase of σ_e, whose maximum deviation reached 2.3%. The graphical representation of the $\Delta\sigma_e$ function in variables (h_d, γ) can be seen in Fig. 17. The diagram is a qualitative replica of the surface derived for $S_{Hmax} = S_{hmin} = 16$ MPa.

Comparing the σ_e^0 values for different horizontal stress ratios against variation $\Delta\sigma_e$ for the $S_{Hmax} > S_{hmin}$ case, we came to a conclusion that stress heterogeneity had a greater effect on rock failure than the colmatation zone.

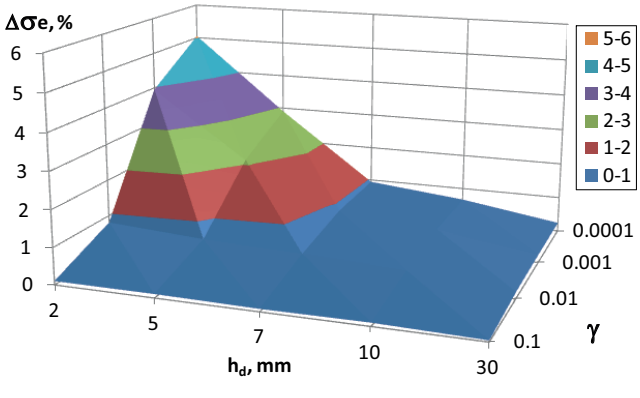

Fig. 15. Deviation of the maximum values of equivalent stresses in the near-welbore area in the homogeneous field of horizontal stresses $S_{Hmax} = S_{hmin} = 16$ MPa in dependence on the width h_d and the colmatation zone permeability k_d. The parameter γ is a quantitative characteristic of permeability reduction when compared to the uninvaded formation ($k_d = \gamma k$)

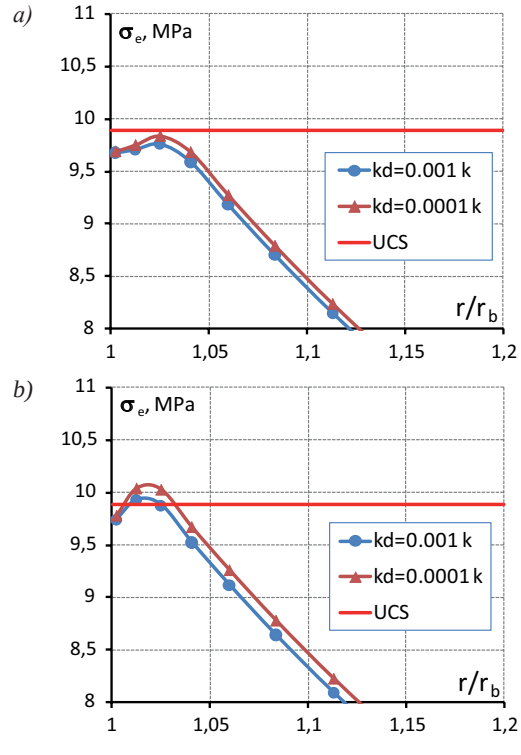

Fig. 16. The σ_e function distribution in the near-well area for h_d = 5 mm (a) and h_d = 2 mm (b), horizontal stresses $S_{Hmax} = S_{hmin} = 16$ MPa, dP = 4 bar, relative section depth h = 0.5 m, and well radius r_b = 0.11 m

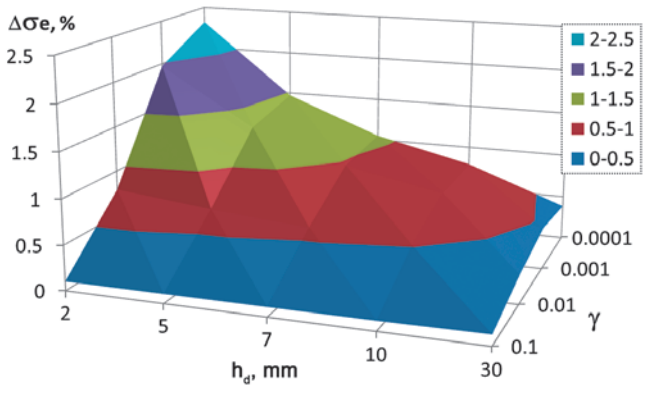

Fig. 17. Deviation function built for S_{Hmax} = 18.55 MPa, S_{hmin} =17.5 MPa in the dependence on the colmatation zone width h_d and the permeability reduction factor γ

Conclusions

Generalizing of the results obtained for the Vadelypskoye oil field has brought us to the following conclusions:

1. The modeling has confirmed sand production during water pumping from the reservoir at the pressure drawdown of 4-6 bar.

2. In the presence of homogeneous horizontal stresses, the following operation modes can be considered as safe:

- pressure drop down to 6 bar is acceptable at the horizontal stresses of 15 MPa and in the presence of a moderately contaminated (10-20% of formation's permeability) near-wellbore area;

- pressure drop down to 4 bar is acceptable at the horizontal stresses of 17 MPa and in the presence of a moderately contaminated near-wellbore area.

3. Under the borehole conditions when the maximum horizontal stress exceeds the minimum one by 1.05 MPa for cases S_{hmin} = 15 MPa, S_{Hmax} = 16 MPa; and S_{hmin} = 17.5 MPa, S_{Hmax} = 18.55 MPa in the presence of a moderately contaminated near-wellbore area, sanding begins at the pressure drawdown of 4 bar.

4. The effect of near-well contamination degree and its width on equivalent stress increasing is most apparent in the presence of homogeneous horizontal stresses and may reach up to 6% of the equivalent stress level calculated for water extraction from a noncontaminated formation.

5. Highly-impermeable colmatation zones of 2-5 mm in length produce a high pore pressure gradient while water lift that causes cylindrical pieces (1-2 mm) to scale off from borehole walls. This effect can be observed in the presence of homogeneous horizontal stresses.

6. Changing of the colmatation- zone parameters in a field of horizontal stresses may increase the equivalent stress up to 2.5% relative to the one calculated for water pumping from a noncontaminated formation.

7. Analysis of transition from homogeneous horizontal stresses to heterogenous ones with account for a destruction function for the near-well area demonstrates that the equivalent stress is more sensitive to a difference between horizontal stresses rather than to colmatation zone parameters.

Recommendations for drilling and operation of water-supply wells at the field

The obtained results have enabled us to formulate the following recommendations:

1. Use sand screens with the cell diameter of 0.1 mm.

2. When penetrating a target horizon use a drill mud whose particles are bigger than the pore size to prevent damage zone formation.

3. Use a drilling mud with low concentration of suspended particle to form a permeable colmatation zone. This drilling mode provides a non-increasing of the equivalent stress on the wall under subsequent water pumping.

4. If using suspensions is critical for preventing mud from entering into inferior oil-saturated layers, we recommend using fine-dispersed fractions to form an extended colmatation zone, which, however, may complicate water extraction.

5. Produce water from a formation with the heterogenous horizontal stresses of about 15 MPa, apply the pressure drawdown of no more than 6 bar.

6. Produce water from a formation with the heterogenous horizontal stresses of about 17 MPa, apply the pressure drawdown of no more than 4 bar.

7. Pay special attention to determining actual horizontal stresses in the formation, since the amount of maximum horizontal stress exceeding over the minimum one has a more significant effect on rock failure while water extraction than colmatation zone formation while drilling.

References

Biot M.A. (1941). General Theory of Three-Dimensional Consolidation. *Journal of Applied Physics*, 12(2), pp. 155-161. https://doi.org/10.1063/1.1712886

Biot M.A., Willis D.G. (1957). The Elastic Coefficients of the Theory of Consolidation. *Journal of Applied Mechanics*, 24, pp. 594-601.

Bocharov O.B., Serjakov A.V. (2016). Modelirovanie neharakternogo razrushenija produktivnyh sloev peschanika pri burenii [Simulation of uncharacteristic destruction of sandstone productive layers during drilling]. *Fizicheskaya Mezomehanika = Physical Mesomechanics Journal*, 19(6), pp. 86-93. (In Russ.)

Chang C., Zoback M. D. and Khaksar A. (2006). Empirical relations between rock strength and physical properties in sedimentary rocks. *Journal of Petroleum Science and Engineering*, 51, pp. 223-237. https://doi.org/10.1016/j.petrol.2006.01.003

Fjær E., Holt R.M., Horsrud P., Raaen A.M. and Risnes R. (1992). Petroleum Related Rock Mechanics. *Developments in Petroleum Science*, 33, 337 p.

GMI SFIB User's manual (2008). GeoMechanics International, Inc., 295 p.

Manakov A.V., Rudjak V.Ja. (2012). Algoritm sovmestnogo modelirovanija fil'tracionnyh i geomehanicheskih processov v priskvazhinnoj zone [Algorithm for joint modeling of filtration and geomechanical processes in the near-wellbore

zone]. *Sibirskiy zhurnal industrialnoy matematiki = Siberian Journal of Industrial Mathematics*, 15, 1(49), pp. 53-65. (In Russ.)

Podberezhny M., Polushkin S., Makarov A. (2017). Novel Approach for Evaluation of Petrophysical Parameters from Time-lapse Induction Logging-While-Drilling Measurements in Deviated and Horizontal Wells. *Proceedings of the SPE Russian Petroleum Technology Conference*, Moscow, Russia. SPE-187911-MS. https://doi.org/10.2118/187911-MS

Wang H.F. (2000). Theory of Linear Poroelasticity with Applications to Geomechanics and Hydrology. Princeton: Princeton University Press, 287 p.

Zienkiewicz O. (1975). Metod konechnyh elementov v tehnike [The finite element method in engineering science]. Moscow: Mir, 544 p. (In Russ.)

About the Authors

Alexander V. Seryakov – Researcher, PhD (Engineering)

Novosibirsk Technology Center Baker Hughes JSC

4A, Kutateladze st., Novosibirsk, 630090, Russian Federation

E-mail: Alexander.Seryakov@bakerhughes.com

Maxim Yu. Podberezhny – Chief petrophysicist, PhD (Physics and Mathematics)

Salym Petroleum Development NV

31, Novinsky boul., Moscow, 123242, Russian Federation

Oleg B. Bocharov – PhD (Physics and Mathematics), Deputy Director

Novosibirsk Technology Center Baker Hughes JSC

4A, Kutateladze st., Novosibirsk, 630090, Russian Federation

Marat A. Azamatov – Head of the Department, Master of Physics, MSc Petroleum Engineering

Salym Petroleum Development NV

31, Novinsky boul., Moscow, 123242, Russian Federation

Manuscript received 31 July 2018;
Accepted 26 September 2018;
Published 30 November 2018